Histochem Cell Biol (1996) 105:179–185

ORIGINAL PAPER

Anja-Rose Strohmaier · Herbert Spring
Eberhard Spiess

Three-dimensional analysis of the substrate-dependent invasive behavior of a human lung tumor cell line with a confocal laser scanning microscope

Accepted: 20 November 1995

Abstract Matrigel and collagen G gels were used as models for basement membrane and interstitial space-collagen, respectively, to study the invasive behavior of cells of the human lung tumor cell line EPLC 32M1, which was derived from a squamous cell carcinoma. For three dimensional analysis of the invasive process, cells were seeded onto the gels in a slide chamber and observed with a confocal laser scanning microscope. Optical sectioning in the *xy* and *xz* directions and image reconstruction with computer programs allowed us readily to obtain a three-dimensional overview of the invasive process in situ. Both types of gel showed a smooth surface. Matrigel had a granular structure whereas collagen G revealed a fiber-like morphology. The tumor cells showed a matrix-dependent behavior. On Matrigel, within 24 h of incubation, a network of cells appeared on the surface, which developed further within 72 h to interconnected multicellular cords also invading the gel. Tumor cells seeded on collagen G remained individual. They formed pseudopodia and achieved tight contact with the matrix, eventually also invading the gels in a time-dependent manner. Therefore, the composition of the substrate crucially influences the invasion path.

Introduction

The main characteristics of malignant tumor cells are their ability to invade through tissue barriers into the host tissue and to disseminate and form metastases at distant sites. The complex process of invasion in an extracellular matrix can be separated into three steps: (1) attachment of tumor cells to the matrix; (2) degradation of the matrix by proteolytic and/or glycolytic enzymes; and (3) invasion of cells into the target tissue (Liotta 1986; Sloane et al. 1990; Mignatti and Rifkin 1993; Stetler-Stevenson et al. 1993). Basal membranes and connective tissue are the most important barriers for tumor cells in this dissemination process. Therefore, different types of in vitro models have been developed to elucidate the invasiveness of tumor cells using reconstituted basement membrane, e.g., Matrigel or interstitial collagen-like collagen compositions (Liotta et al. 1980; Kramer et al. 1986; Albini et al. 1987; Montcourrier et al. 1994).

To study the morphology and behavior of cells in such models conventional light microscopy, scanning or transmission electron microscopy has been used (Boxberger et al. 1989; Noël et al. 1991; Azuma et al. 1994; Kuzuya and Kinsella 1994). We used the technique of confocal laser scanning microscopy together with a slide chamber. This combination enabled us to create a three-dimensional image of the invasive process. These images cannot be so readily and reproducibly produced by other techniques. Furthermore, we minimized the risk of artifacts provoked by extensive fixation, staining and embedding protocolls, and by mechanical sectioning. In this study we describe the invasive behavior of the human lung tumor cell line, EPLC 32M1 (undifferentiated squamous cell carcinoma), in Matrigel and collagen, substituting basal membrane and interstitial collagen, respectively.

A.-R. Strohmaier · H. Spring · E. Spiess (✉)
Biomedizinische Strukturforschung (0195),
Deutsches Krebsforschungszentrum, Im Neuenheimer Feld 280,
D-69120 Heidelberg, Germany
Tel. +49-6221-423426; Fax +49-6221-423459

Materials and methods

Cells and cultures

The epidermoid human lung cancer cell line, EPLC 32M1, derived from a squamous cell carcinoma (Bepler et al. 1988; Heidtmann et al. 1992) has been studied. Cells were cultured in RPMI 1640 medium supplemented with 10% fetal bovine serum, 6 mM L-glutamine and 0.22% sodium bicarbonate (Biochrom, Berlin, Germany; full medium) in a humidified atmosphere of 5% CO_2 at 37° C. Cells grown as monolayers were detached by exposure to 0.02% EDTA (Merck, Darmstadt, Germany) in phoshate-buffered saline (PBS: 140 mM NaCl, 50 mM KCl, 8 mM Na_2HPO_4, 1.5 mM KH_2PO_4, pH 7.2).

Preparation of the slide chambers

Special slide chambers with a glass coverslip as the bottom for studying cells directly and without multiple preparation steps were

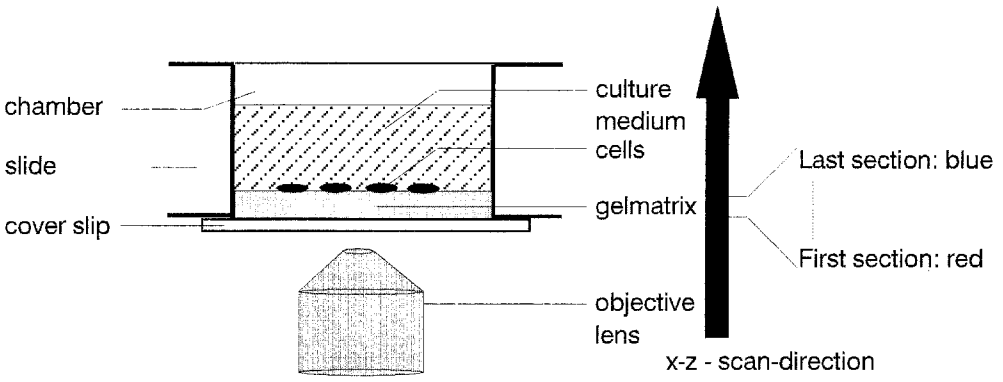

Fig. 1 Vertical section of the slide chamber used to study the behavior of 32M1 cells. The direction of sectioning defined by the system software is indicated at the right. For depth reconstruction images, the color codes of the first and the last section are added. Chamber, cells, and objective are not to the same scale

constructed (Fig. 1) according to Spring and Franke (1981). Coverslips were cleaned for 15 min in an ultrasonic bath with a 1:1:1 mixture of chloroform:ethanol:petrol ether. The holes in a 5-mm-thick plastic slide were sealed on the bottom with coverslips. A two-component paste (Uhu, Bühl, Germany) was used for that procedure. The slide chambers were baked for 60 min at 60° C, washed in ethanol, and incubated overnight at 37° C with full medium. After washing again with ethanol, the chambers were air-dried in a sterile horizontal flow bench. A block of paraffin was rubbed on the inner sidewall of the chambers. This water-repellent treatment is essential to obtain an even gel surface (Imamura et al. 1994).

Preparation of the gels

Two different types of gels were used for the experiments described. We used Matrigel (Collaborative Research, Bedford, Mass., USA) as a model for the basal membrane. Matrigel is a solubilized basement membrane preparation extracted from the Engelbreth-Holm-Swarm mouse sarcoma tumor. Its major components are laminin, collagen type IV, and heparan sulfate proteoglycan. It also contains traces of a number of growth factors. The gel solution was thawed on ice and handled with precooled and shortened pipette tips. The fluid gel solutions (40 µl) were pipetted onto the bottom of the chambers and were allowed to polymerize at 37° C for 30 min. As a model for the interstitial matrix we used collagen G (Biochrom). This is extracted from calfskin collagen and consists of 90% collagen type I and 10% collagen type III. We mixed eight parts of collagen G with one part 7.5% NaCl and one part 0.2 N NaOH in 200 mM HEPES, pH 12.0. The preparation of the gels was similar to that of Matrigel. The polymerized gels had a thickness of approximately 100–300 µm.

Invasion assay

A total number of 25×10^3 cells in 500 µl full medium was seeded in each chamber, incubated for 24 h and then fixed with 1% paraformaldehyde in PBS for 10 min. For detection, the cells were stained for 5 min with 1 µg/ml of the fluorescent dye 3,3′-dihexyloxacarbocyanine iodide [$DiOC_6$ (3), Molecular Probes, Eugene, Ore., USA] dissolved in PBS.

Confocal laser scanning microscopy

Confocal laser scanning microscopy was performed using an inverse LSM 410 UV (Carl Zeiss, Jena, Germany) with an argon-ion laser for the excitation wavelength of 488 nm. A water-immersion objective (C-Apochromat 40×/1.2 W Korr; Zeiss) was used. The two main advantages of this objective are that the water immersion results in high contrast and resolution, and that the long working distance of 220 µm is ideal for thick specimens.

Optical sections were created in the planar (*xy*) and axial (*xz*) directions. Horizontal scales were automatically calculated by the system software. To obtain vertical scales, it has to be considered that the axial distances between the scanned pixels are variable in the specimen but invariant in the pixel matrix of the screen. Therefore, the images may show a stretched or compressed picture of the specimen. Additionally, the software was programmed with the refractive indices for Matrigel and collagen G (n=1.335 and 1.337, respectively, as determined by refractometry) and presents these data as *xy*/*xz* scale ratios, which can be used to calculate the absolute *xz* scale values. These have been included as vertical bars where appropriate.

As we used an inverse microscope, the procedure of sectioning determined by the system always started at the bottom of the chamber. Three-dimensional image reconstructions of consecutive *xy* sections were generated by the system software. In these reconstructions the depth of the section is coded by different colors. The bottom of the chamber (starting at section zero) is coded in red and the top of the gel (final section) in blue (Fig. 1).

Results

Morphology of Matrigel and collagen G

The stain $DiOC_6$ (3), which was used to visualize the cells, also stained Matrigel. After incubation under cell culture conditions for 24 h and staining with $DiOC_6$ (3), Matrigel showed a granular structure in all dimensions and a smooth gel surface when analyzed in the fluorescent mode (Fig. 2A, B).

Under the same conditions, the collagen G gel remained unstained. But the surface of the gel and its structure could be visualized in the reflection mode of the confocal laser scanning microscope (CLSM). The surface of this gel was as smooth as the surface of Matrigel (Fig. 2C). Instead of granular structures, the gel consisted of fibers. In the *xz* sections these resembled Matrigel, but the *xy* sectioning (Fig. 2D) clearly revealed the fiber-like structure. This indicates a predominant *xy* orientation of collagen fibers. The apparent differences in signal density of Matrigel and collagen G might therefore, depend not only on the different modes of visualization but also on the actual differences in density.

Morphology and invasive behavior of 32M1 cells

In plastic flasks, individual cells were spread and elongated with a bulge around their nucleus. In monolayers,

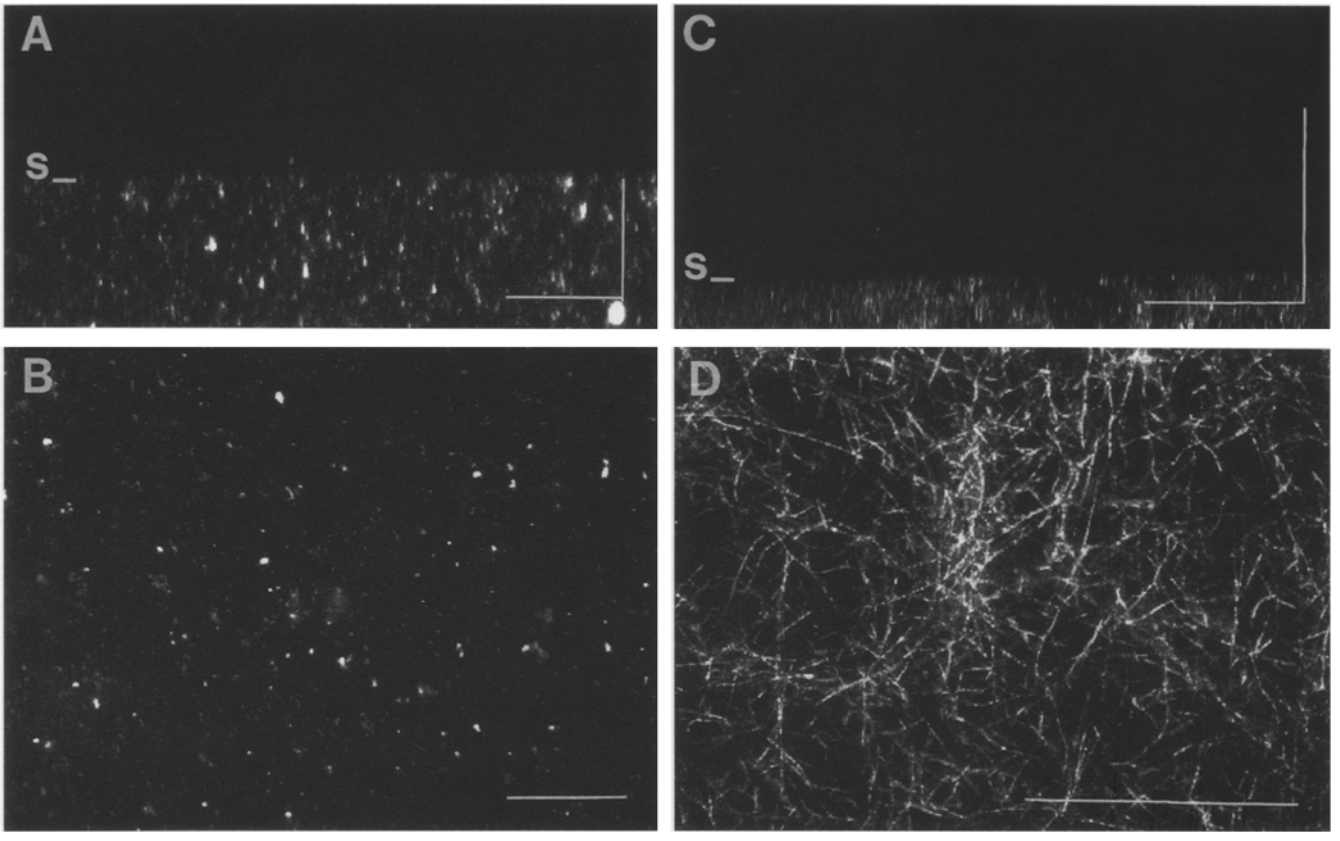

Fig. 2A–D Morphology by laser scanning microscopy of Matrigel and collagen G after 24 h incubation without cells and 10 min fixation with 1% paraformaldehyde. Matrigel: stained with 1 µl/ml 3,3′-dihexyloxacarbocyanine iodide in phosphate-buffered saline for 5 min and visualized in the fluorescence mode. **A** Line scan section in the *xz* direction. **B** Section in the *xy* direction. Collagen G: visualized in the reflection mode. **C** Line scan section in the *xz* direction. **D** Section in the *xy* direction. The surface of the gel is indicated by *s*. Horizontal and vertical *scale bars* represent 50 µm

cells became more compact and the layer itself had a cobblestone morphology.

Matrigel

One hour after seeding, the cells were spread out and individual. After 3 h they had gathered into small clusters consisting of two to five cells, and after 24 h they had formed cord-like structures interconnected to a network-like layer of cells (Fig. 3A). In the middle of the aggregates on Matrigel, cells had the same spherical shape as cells in a monolayer, whereas inside the cords they were elongated (Fig. 3B). From the cord formation we conclude that the cells were excessively migrating in a cooperative process. Optical CLSM sections in the *xz* direction after 24 h of incubation showed that the cords and aggregates consisted largely of multi-cell layers (Fig. 3C). In the dense parts of the network, up to three layers were formed within 24 h and increasing thickness was observed with longer incubation time (72 h). The surface of the gel, originally very smooth, was deformed and the cells were partly embedded in the gel and cords developed downward into the gel, as shown with the *xz* sections (Fig. 3D). This invasion is clearly documented by a three-dimensional reconstruction obtained from 16 *xy* sections (Fig. 4A). Only cells that were part of the network could be found in the interior of the gels, whereas single cells or cell clusters detached from the network were not observed to invade the gels. The process of invasion continued and, after 72 h, the cell layer had become thick and extended into the gel (Fig. 3E).

Collagen G

On collagen G, the cells developed pseudopodia within 3 h of seeding. A fraction of the cells exhibited the typical elongated, polarized morphology of locomotive cells, having a leading pseudopodium (Fig. 4B, C), but no accumulations were observed during incubation. Some cells formed particularly long pseudopodia, stretching either horizontally (Fig. 4B) or even downwards into the gel (Fig. 4C).

Using the reflection and fluorescence modes it was possible to study both the gel and the cells simultaneously (Fig. 4D–F). The cells seemed to achieve tight contact with the matrix and to organize the collagen fibers around themselves.

By simultanous reflection and fluorescent mode microscopy, *xz* sectioning proved that single cells invaded the gel. After 24 h of incubation, cells inside the gel could

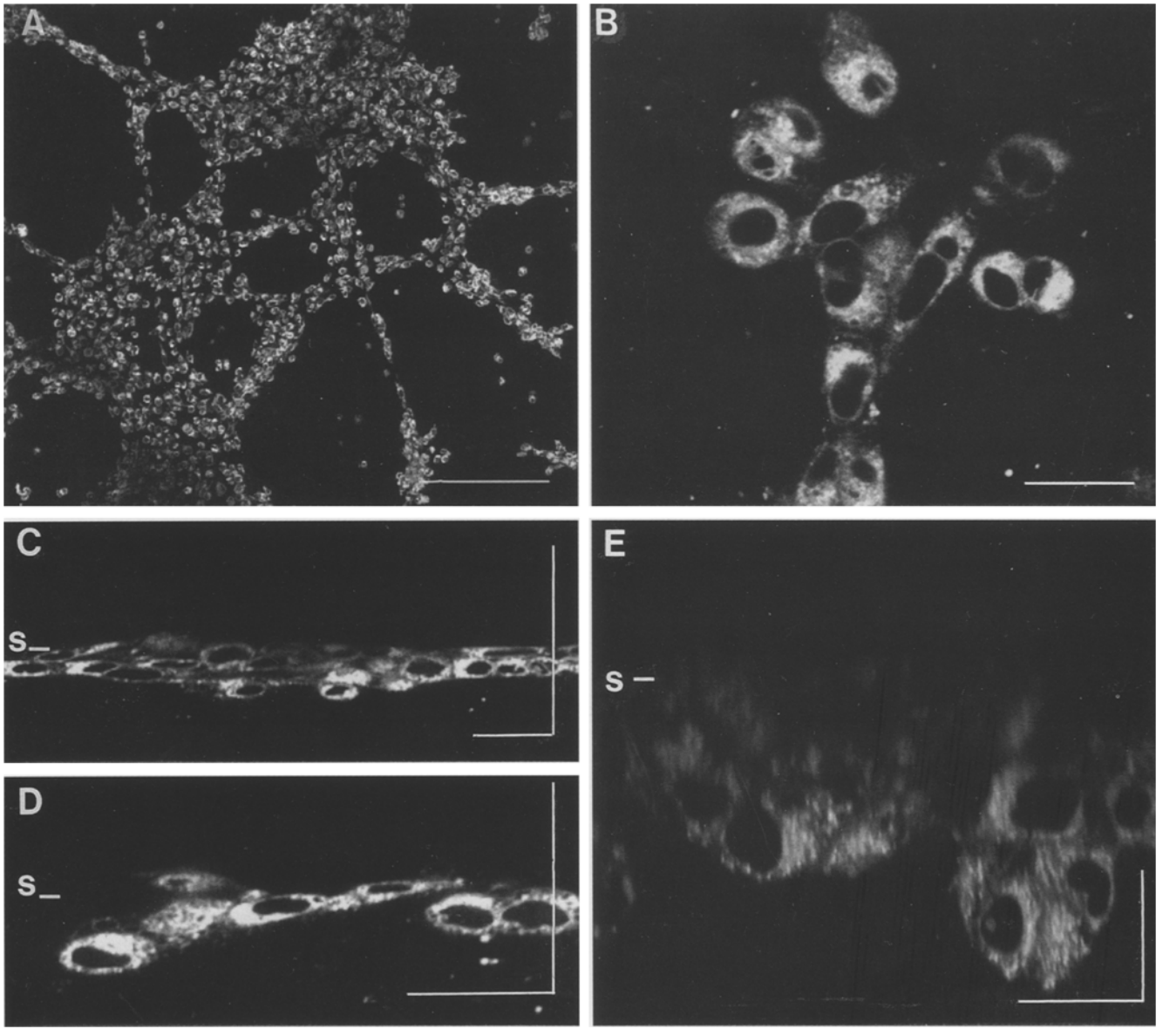

Fig. 3 Morphology and invasive behavior of 32M1 cells on Matrigel by fluorescent laser scanning microscopy after 24 (**A–D**) and 72 h (**E**) of incubation. **A** Section in the *xy* direction of the network-like cell layer. **B** Section in the *xy* direction. **C–E** Line scan sections in the *xz* direction. *Bars* in **A** and **B** represent 100 µm and 25 µm, respectively. Horizontal and vertical *bars* in **C–E** represent 25 µm. The surface of the gel is indicated by *s*

be observed (Fig. 4E). The cells continued their invasion and, after 72 h, more cells had invaded and cells were found that had penetrated the gel more deeply (Fig. 4F).

The three-dimensional reconstruction of a stack of 16 sections shows single cells about 40 µm deep inside the gel (Fig. 4C).

Discussion

In this study we visualized the behavior of invasion of 32M1 lung tumor cells on two different substrates with the aid of CLSM. There are several problems which have to be considered when studying invasion of cells by conventional light or electron microscopy. The preparation and fixation of the specimens include a number of steps, leading to artifacts. We used a special slide chamber in combination with CLSM to study the cells. This procedure has the advantage that the complete observation is done in situ, including only one step of mild fixation (1% paraformaldehyde). In addition, CLSM allows destruction-free optical sectioning and three-dimensional reconstruction.

The clear visualization of cells depends on the combination of the applied microscopical device and the staining method. By use of a long-distance water-immersion objective we obtained exceptionally clear and high-resolution images. In CLSM, fluorescent staining is necessary to visualize whole cells by the confocal principle in a three-dimensional way. We introduced the membrane-staining carbocyanin, $DiOC_6$ (3); it is easy to apply and

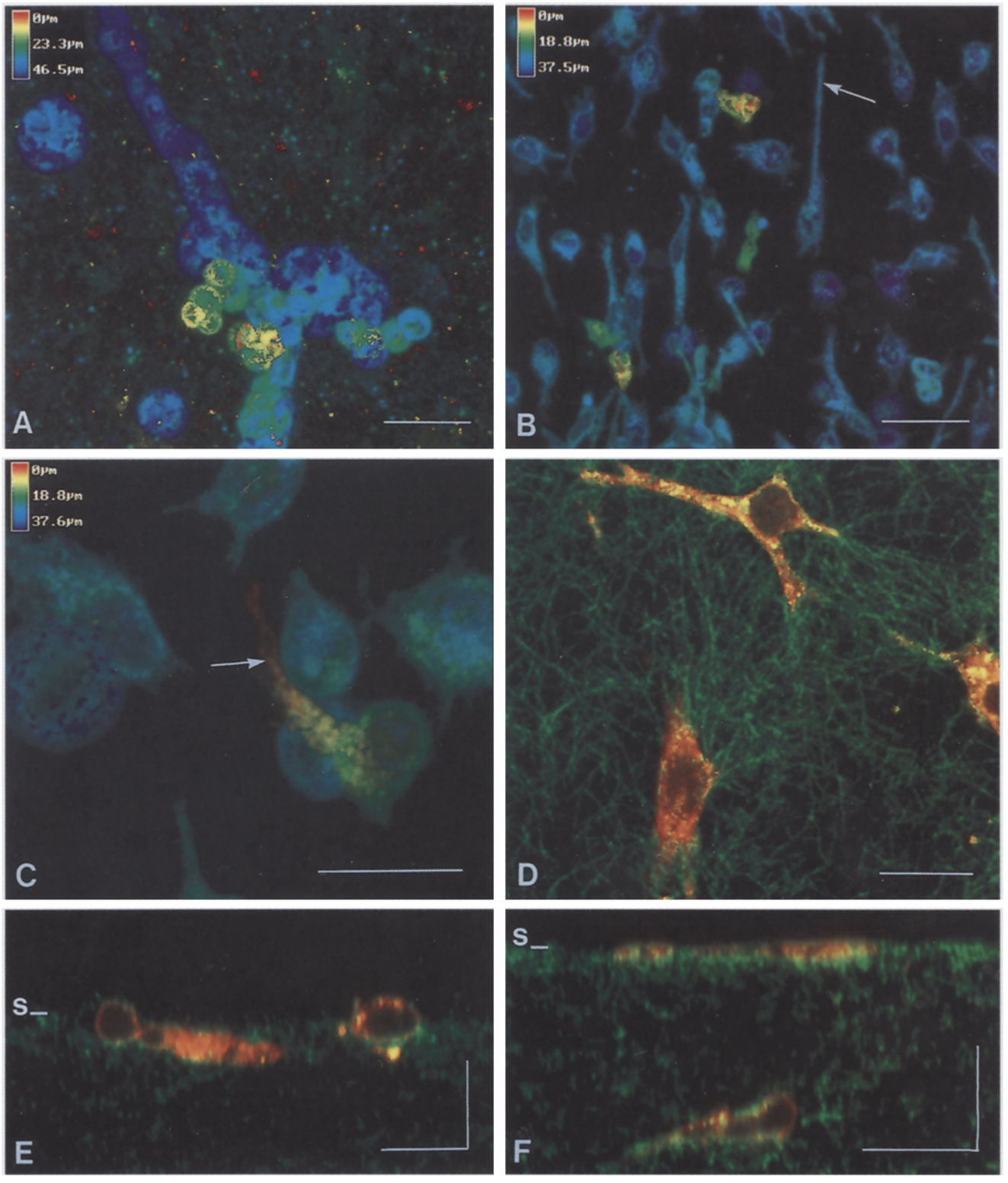

Fig. 4 **A** Morphology and invasive behavior of 32M1 cells on Matrigel after 24 h of incubation by fluorescent laser scanning microscopy. Image reconstruction of 16 single *xy* sections; the surface of the gel (last section) is given in blue, the bottom of the gel (first section starting with zero) in red. **B–F** Morphology and invasive behavior of 32M1 cells on collagen G. **B** and **C** are image reconstructions of 16 single *xy* sections taken after 24 h of incubation in the fluoresecent mode. The color coding is as described for **A**. **D–F** Sections through cells taken by combination of reflection mode (green) and fluorescent mode (red). **D** *xy* section. **E**, **F** *xz* line scan sections. The surface of the gel is indicated by *s*. *Bars* in **A** and **B** represent 50 µm; *bars* in **C–E** 25 µm for both horizontal and vertical scales

provides high staining efficiency. Due to its spectral characteristics it potentially faciliates multiplex staining. In order to achieve higher resolution and contrast we used slide chambers with glass bottoms instead of the 6- or 24-well plastic plates routinely used in cell culture.

By fluorescent or reflection modes we could clearly visualize the different morphological characters of the applied gels. Basement membranes consisted of a network of filaments (Inoué et al. 1983). The scaffolds were highly cross-linked collagen IV fibers which supported the matrix with mechanical stability (Martin and Timpl 1987). The observed granules are probably complexes of proteoglycan and laminin (Kleinman et al. 1986). The network of collagen type IV could neither be observed in the fluorescent nor in the reflection mode. The collagen G gel clearly revealed the readily recognizable collagen fibers.

The behavior of the 32M1 cells was clearly substrate dependent. On both biological substrates the morphology was different and was also different from that on the plastic of cell culture flasks. On contact with Matrigel the cells formed networks consisting of thick cords; this process requires cell migration. The cord formation must be a cooperative process as cords became thicker and the meshwork wider, rather than a more filigree-like network. This cooperativity is also obvious in the vertical growth of cords: we never observed individual cells inside the gel. It is not yet clear what influence the traces of growth factors exert on the cells. Similar morphological phenomena were also described for other cell types. Kubota et al. (1988) showed that cultivation on Matrigel provoked tube formation by endothelial cells, which even exhibited real lumina. The cords created by the 32M1 cells are pseudotubular structures because they exhibited no lumen. Spanel-Borowski et al. (1994) observed the formation of similar pseudotubular structures for cytokeratin-positive endothelial cells derived from bovine aorta and vena cava. Kramer et al. (1986) observed migration and the creation of a three-dimensional network by fibrosarcoma cells. The 32M1 cells migrated on the Matrigel, but we found no pseudopodia under these conditions. This is in contrast to the general finding that movement is associated with the bipolarity of cells having one prominent leading pseudopodium (Lee et al. 1993).

On collagen G, a mixture of collagen type I and type III, we observed no cord formation, but individual cells which invaded the gel. The 32M1 cells exhibited a similar behavior to capillary endothelial cells on interstitial collagen: they adhered and spread. In contrast, cords were formed in contact with extracts from basal membranes (Madri et al. 1983). A fraction of cells showed a leading pseudopodium reaching deep into the gel. This indicates that these cells started the penetration of the collagen gel with a pseudopodium and the body of the cell follows into the channel carved.

Both types of model matrices revealed the invasive character of the cells. The composition of the matrix crucially influences their path of invasion.

Kramer et al. (1986) related the invasive behavior of fibrosarcoma cells HT180 in vitro to the malignant phenotype in vivo. Results of Simon et al. (1992) show, however, that the capacity of cells to migrate through Matrigel does not universally correlate with the in vivo invasive activities of different types of cells. The 32M1 cells provoked the growth of tumors and distant metastases in nude mice after intraperitoneal injection (Heidtmann et al. 1992). In this case, the in vitro behavior correlates with the results of the in vivo experiments.

The ability to invade through anatomical barriers into normal adjacent tissues presupposes that tumor cells are equipped with proteolytic enzymes for the destruction of the surrounding extracellular matrix. Enzymes belonging to the different groups of serine proteases as well as metalloproteinases and cysteine proteinases (cathepsins) are involved in this process (Sloane et al. 1990; Mignatti and Rifkin 1993). 32M1 cells are known to express plasminogen activators (Heidtmann et al. 1989) as well as cathepsins B and L (Ulbricht et al. 1995). Therefore, we can take our observations of perturbations and rearrangements of both substrates as an indication of enzymatic activities exhibited by the tumor cells. Our approach combining CLSM and slide chambers opens a variety of possibilities to investigate further those factors influencing the process of invasion and the visualization of invading cells.

Acknowledgements This investigation was supported by the Klinisch-Biomedizinischer Forschungsverbund of the Bundesministerium für Forschung und Technologie, Germany and a grant of the DKFZ-NCRD Cooperation in Cancer Research (E. Spiess, A.-R. Strohmaier).

References

Albini A, Iwamoto Y, Kleinman HK, Martin GR, Aaronson SA, Kozlowski JM, McEwan RN (1987) A rapid in vitro assay for quantitating the invasive potential of tumor cells. Cancer Res 47:3239–3245

Azuma M, Tamatani T, Fukui K, Bando T, Sato M (1994) Enhanced proteolytic activity is responsible for the aberrant morphogenetic development of SV40-immortalized normal human salivary gland cells grown on basement membrane components. Lab Invest 70:217–227

Bepler G, Köhler A, Kiefer P, Havemann K, Beisenherz K, Jaques G, Gropp C, Haeder M (1988) Characterisation of the state of differentiation of six newly established human non-small-cell lung cancer cell lines. Differentiation 37:158–171

Boxberger H-J, Paweletz N, Spiess E, Kriehuber R (1989) An in vitro study of Bsp73 rat tumor cell invasion into endothelial monolayer. Anticancer Res 9:1777–1786

Heidtmann HH, Hofmann M, Jacob E, Erbil C, Havemann K, Schwartz-Albiez R (1989) Synthesis and secretion of plasminogen activators and plasminogen activator inhibitors in cell lines of different groups of human lung tumors. Cancer Res 49:6960–6965

Heidtmann HH, Elsässer HP, Salge U, Hejmanns J, Erbil C, Schwartz-Albiez R, Havemann K (1992) Plasminogen activator system and xenograft growth patterns in human non-small-cell lung cancer cell lines. Fibrinolysis 6 [Suppl 4]:77–82

Imamura H, Takao S, Aikou T (1994) A modified invasion -3-(4,5-dimenthylthiazole-2-yl)-2,5-diphenyltetrazolium bromide assay for quantitating tumor cell invasion. Cancer Res 54:3620–3624

Inoué S, Leblond CP, Laurie GW (1983) Ultrastructure of Reichert's membrane, a multilayered basement membrane on the parietal wall of the rat yolk sac. J Cell Biol 97:1524–1537

Kleinman HK, McGarvey ML, Hassel JR, Star VL, Cannon FB, Laurie GW, Martin GR (1986) Basement membrane complexes with biological activity. Biochemistry 25:312–318

Kramer RH, Bensch KG, Wong J (1986) Invasion of reconstituted basement membrane matrix by metastatic human tumor cells. Cancer Res 46:1980–1989

Kubota Y, Kleinman HK, Martin GR, Lawley TJ (1988) Role of laminin and basement membrane in the morphological differentiation of human endothelial cells into capillary-like structures. J Cell Biol 107:1589–1598

Kuzuya M, Kinsella JL (1994) Induction of endothelial cell differentiation in vitro by fibroblast-derived soluble factors. Exp Cell Res 215:310–318

Lee J, Ishihara A, Jacobson K (1993) How do cells move along surfaces? Trends Cell Biol 3:366–370

Liotta LA (1986) Tumor invasion and metastases: role of extracellular matrix. Rhoads Memorial Award Lecture. Cancer Res 46:1–7

Liotta LA, Lee WC, Morakis DJ (1980) New method for preparing large surfaces of intact basement membrane for tumor invasion studies. Cancer Lett 11:141–152

Madri JA, Williams SK, Wyatt T, Mezzio C (1983) Capillary endothelial cell cultures: phenotypic modulation by matrix components. J Cell Biol 97:153–165

Martin GR, Timpl R (1987) Laminin and other basement membrane components. Annu Rev Cell Biol 3:57–85

Mignatti P, Rifkin DB (1993) Biology and biochemistry of proteinases in tumor invasion. Physiol Rev 73:161–195

Montcourrier P, Mangeat PH, Valembois C, Salazar G, Sahuquet A, Duperray C, Rochefort H (1994) Characterization of very acidic phagosomes in breast cancer cells and their association with invasion. J Cell Sci 107:2381–2391

Noël AC, Callé A, Emonard HP, Nusgens BV, Simar L, Foidart J, Lapiere CM, Foidart J-M (1991) Invasion of reconstituted basement membrane matrix is not correlated to the malignant metastatic cell phenotype. Cancer Res 51:405–414

Simon N, Noël A, Foidart J-M (1992) Evaluation of in vitro reconstituted basement membrane assay to assess the invasiveness of tumor cells. Invasion Metastasis 12:156–167

Sloane BF, Moin K, Krepela E, Rozhin J (1990) Cathepsin B and its endogenous inhibitors: the role in tumor malignancy. Cancer Metastasis Rev 9:333–352

Spanel-Borowski K, Ricken A, Patton WF (1994) Cytokeratin-positive and cytokeratin-negative cultured endothelial cells from bovine aorta and vena cava. Differentiation 57:225–234

Spring H, Franke WW (1981) Transcriptionally active chromatin in loops of lampbrush chromosomes at physiological salt concentrations as revealed by electron microscopy of sections. Eur J Cell Biol 24:298–308

Stetler-Stevenson WG, Liotta LA, Kleiner DE (1993) Extracellular matrix: role of matrix metalloproteinase in tumor invasion and metastasis. FASEB J 7:1434–1441

Ulbricht B, Spiess E, Schwartz-Albiez R, Ebert W (1995) Quantification of intracellular cathepsin activities in human lung tumor cell lines by flow cytometry. Biol Chem. Hoppe Seyler 376:407–414